

Received October 14, 2017; reviewed; accepted February 3, 2018

## Galvanic contacting effect of pyrite on xanthate adsorption on galena surface: DFT simulation and cyclic voltammetric measurements

Baolin Ke <sup>2</sup>, Jianhua Chen <sup>1,3</sup>, Yuqiong Li <sup>1</sup> and Ye Chen <sup>3</sup>

<sup>1</sup> Innovation Center for Metal Resources Utilization and Environment Protection, Guangxi University, Nanning 530004, P.R. China

<sup>2</sup> Mining College, Guizhou University, Guiyang 550025, P.R. China

<sup>3</sup> School of Resources, Environment and Materials, Guangxi University, Nanning 530004, P.R. China

Corresponding author: [jhchen@gxu.edu.cn](mailto:jhchen@gxu.edu.cn) (Jianhua Chen)

**Abstract:** The effect of galvanic interaction between pyrite and galena on xanthate adsorbing on the galena surface has been investigated by means of density functional theory (DFT) and cyclic voltammetric measurements. The calculated results show that differences in the contact site and contact distance between galena and pyrite can affect the intensity of the galvanic interaction, and the relationship between the intensity of galvanic interaction and the adsorption ability of xanthate on galena surface has been studied in detail. In general, the galvanic interaction between pyrite and galena surface can enhance the adsorption of xanthate on the galena surface. The adsorption energies of xanthate on the galena surface decrease with the decrease of contact distance, and when the contact distance is lower than 4 Å, the adsorption energies decrease significantly at Pb-Pb, Pb-S and S-S sites. In particular, at the contact distance of 3 Å, a sharp decrease of adsorption energy is observed at the Pb-Pb contact site; in this case, the negative shift of the Pb-S bonding range and DOS non-locality at Pb-Pb contact site are significantly greater than that of the S-S or Pb-S contact sites. The cyclic voltammetric measurements reveal that the galvanic interaction between galena and pyrite improves the adsorption of xanthate on galena surface, which is in good agreement with the DFT results.

**Keywords:** galvanic interaction, adsorption, DFT, pyrite and galena surface, cyclic voltammetric measurements

### 1. Introduction

Sulphide minerals are narrow band gap semiconductors. They are generally found in association with each other in mineral deposits and in the industrial production processes such as metallurgy and flotation, where galvanic interaction could occur between the sulphide minerals due to their different electrode potentials (Cheng and Iwasaki, 1992). It has been known that galvanic interactions play important roles in the generation of acid mine drainage (AMD) (Sadeghiamirshahidi et al., 2013), heavy metal ions pollution (Heidmann and Calmano, 2010), oxidation of sulphide minerals surface (Silva et al., 2003), minerals grinding (Nooshabadi and Rao, 2014), bio-metallurgy (Liu et al., 2007), leaching (Chmielewski and Kaleta, 2011) and flotation (Moslemi et al., 2011).

Sulphide minerals are usually recovered by flotation with xanthate, which is an electrochemical process and exist in a variety of minerals in contact with each other, so that galvanic interaction between the sulphide minerals exerts a strong influence on this flotation process. The electron transfer caused by the galvanic interaction changes the surface properties of sulphides, which will increase or decrease the recovery of the sulphide minerals (Rao S R, 1988). Pyrite has the highest electrode potential among the sulphide minerals while galena has one of the lowest, and therefore, a significant galvanic interaction could occur when these two materials are in contact and make show a marked influence on their flotation (Liu et al., 2009). Qin et al. (2015) used UV spectroscopy to test the

adsorption capacity and rate of butyl xanthate affected by the galvanic interaction between galena and pyrite, and the results suggest that the adsorption of butyl xanthate on the galena surface is enhanced for the galvanic interaction (Qin et al., 2015). However, the microscopic details of the change on agents' adsorption capacity by the effect of galvanic interaction between pyrite and galena have not been well researched by DFT, and the traditional CV test methods could not well directly investigate the effect of galvanic interaction on the agents' adsorption on the single couple mineral.

To further investigate the effect of galvanic interaction between pyrite and galena on xanthate electrochemical adsorption on galena surface, the galvanic interaction models of galena (100) surface with pyrite cluster were constructed, and electrochemical measurement methods have been used in order to obtain further detailed understanding of the galvanic interaction and its effect on the xanthate adsorption on the mineral surfaces.

## 2. Materials and methods

### 2.1 DFT method and models

All calculations were based on the density functional theory (DFT) method and were performed using the CASTEP package, and the GGA-PW91 exchange-correlation functional (Perdew et al., 1992). Only the valence electrons (Fe 3d64S2, Pb 5d106s26p2, S 3s23p4, C 2s22p2, O 2s22p4, H 1s1) were considered through the use of ultrasoft pseudopotentials (Vanderbilt, 1990). A plane wave cut-off energy of 400 eV was used for all calculations. The integration over the Brillouin zone was performed using the Monkhorst-Pack (Monkhorst et al., 1976) scheme, and the number of  $k$  points was set as  $2 \times 2 \times 1$  for all supercell models. The self-consistent field (SCF) convergence tolerance was set to  $2.0 \times 10^{-6}$  eV atom<sup>-1</sup>. The adsorption energies and Mulliken charges calculation methods have been reported by the researches (Li et al., 2018; Ke et al., 2016).

Cluster models have been generally used in DFT calculations of the solid contacting with surface or coating (Ionescu et al., 2003; Li et al., 2013; Roscioni et al., 2013; Shang and Liu, 2010; Zhang et al., 2012). An atomic model of the FeS<sub>2</sub> (100) surface has been used by Herbert et al to investigate the pyrite surface. (Herbert et al., 2014) According to these reports, a cluster model of pyrite (100) (Fe<sub>4</sub>S<sub>8</sub>) has been cleaved from an optimized pyrite (100) surface, and the S1 and S2 atoms of the pyrite cluster were contacted with the galena surface slab model in different contact site, and the contact distances between pyrite cluster and galena surface could also be changed for investigating the galvanic interaction. The "contact distance" using in this paper (such as Figs. 2, 3, 4, 5, 6 etc.) means the distance between S atom of pyrite cluster and the atom of galena surface which interacting with the S atom, which has been used to represent the distance between pyrite cluster and galena surface. The pyrite cluster was constrained during the calculations. A vacuum layer of 25 Å was applied along the  $c$  direction to avoid interactions between the pyrite and bottom surface in the slab. The xanthate molecule has been optimized by the calculating parameters, which are the same as that of the galena surface and pyrite cluster, to make sure the consistency and the correctness of the adsorption energy calculation in this adsorption system.

### 2.2 Cyclic voltammetry measurements

#### 2.2.1 Cyclic voltammetry measurements parameters and mineral samples

Cyclic voltammetry (CV) measurements were performed using a CHI660D-type electrochemical workstation. During this test, saturated calomel electrode and platinum electrode are used as the reference electrode and counter electrode, respectively. The glassy carbon electrodes or the mineral block electrodes are used as the work electrodes. A 0.01 mol/dm<sup>3</sup> sodium borate solution was used as the buffer solution. The experimental parameters were set as follows: scanning area range from -0.8 to 0.8 V, sensitivity of  $10^{-5}$  A/V for glassy carbon electrodes and of  $10^{-4}$  A/V for mineral block electrodes, and the scanning rate of 0.1 V/s. Electrodes were measured in a pH 9.18 buffer solution conditioned with sodium borate, and a 0.001 mol/dm<sup>3</sup> butyl xanthate solution for glassy carbon electrodes while a 0.01 mol/dm<sup>3</sup> butyl xanthate solution was used for mineral block electrodes.

The mineral samples, pyrite (FeS<sub>2</sub>) and galena (PbS), were procured from Guangxi, China. The chemical compositions of the mineral samples are shown in Table 1. The particle of galena and pyrite

samples used for preparing glassy carbon electrodes are ground into below 320 meshes (45  $\mu\text{m}$ ), while the samples used for preparing mineral electrodes are directly cut from the highly mineralized rock samples.

Table 1 Chemical composition of minerals

| Minerals | Composition/ % |       |       |
|----------|----------------|-------|-------|
|          | Pb             | Fe    | S     |
| Galena   | 83.89          | 0.17  | 13.51 |
| Pyrite   | 0.06           | 44.16 | 53.37 |

### 2.2.2 Glassy carbon electrodes preparation and measurements

The surface area of the glassy carbon electrode is a circle with the diameter of 0.3 cm. The method of preparing and examining for glassy carbon electrodes made of galena, pyrite and the mixture of galena and pyrite in the weight ratio of 1:1 using in this paper have been reported by the research (Chen et al., 2015b).

### 2.2.3 Mineral block electrodes measurements

To avoid the mixed effects and to further investigate the galvanic interactions between the minerals, a new electrochemical measurement has been used by Ekmekçi and Demirel (1997). The improved mineral block electrodes using in this paper are based on the above electrochemical measurement, in addition, the electrode 1 is contacted with electrode 2 by a copper wire, which could obtain more stable measurement results. The construction of the improved working electrodes is shown in Fig. 1. It is shown that the block electrode consists of copper wire, resin, silver brazing and mineral. The cylinder minerals with the diameter of 0.55 cm and thickness of 0.3 cm used for preparing mineral electrodes are directly cut from highly mineralized rock samples, and all block electrodes have the same mineral surface area (0.24  $\text{cm}^2$ ).

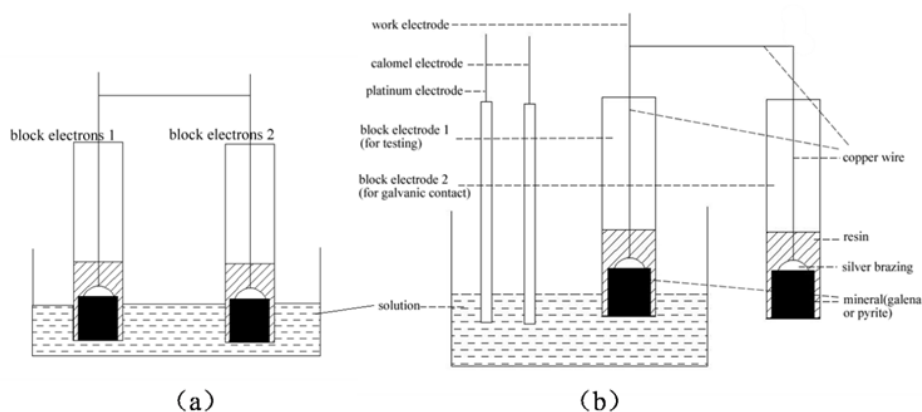


Fig. 1. Diagrammatic drawing of block mineral electrodes CV measurement: (a) before test and (b) testing

Prior to the measurement, first, the mineral block electrodes are ground with alumina powder for 5 min to obtain the fresh mineral surface; and then, the electrode 1 is connected with electrode 2 by a copper wire and both are dipped in the solution for 30 min (shown in Fig. 1(a)), and then taken out to measure. When measuring, the block electrode 1, which is the electrode to be measured, combined with the calomel electrode and platinum electrode, are dipped in the same solution. The block electrode 2, which is connected with block electrode 1 by a copper wire, is placed outside the solution (shown in Fig. 1(b)).

The two block mineral electrodes are alternately used as measured electrodes (electrode 1), and electrode 2 is used to study its galvanic effects on electrode 1 because of the copper wire connection between these two electrodes. When the galena electrode is used as electrode 1, pyrite or galena

electrode is used as electrode 2, while when the pyrite electrode is used as electrode 1, pyrite or galena electrode is also used as electrode 2.

### 3. Results and discussion

#### 3.1 Galvanic interaction between pyrite and galena (100) surface

Pyrite contact with galena (100) surface at the S-S, Pb-S and Pb-Pb sites have been investigated, respectively, and different contact distances between pyrite and galena surface have also been researched. The total numbers of electrons transferred between these galvanic contact interfaces are shown in Fig. 2, and the optimized models are shown in Fig. 3.

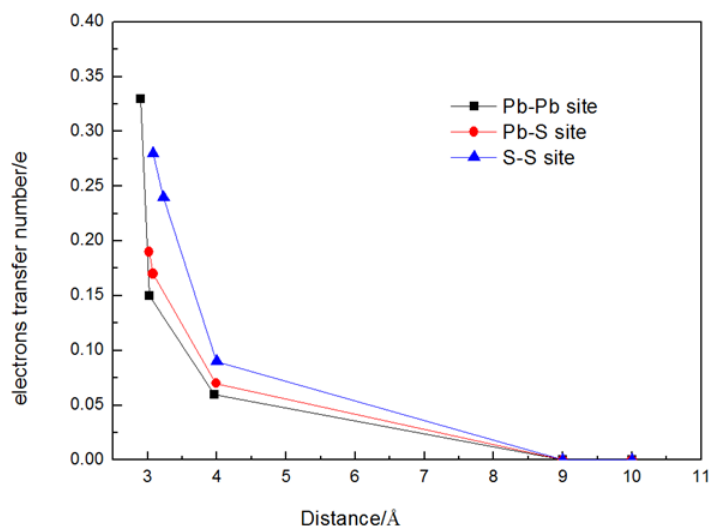


Fig. 2. Total number of electrons transferred from galena surface to pyrite

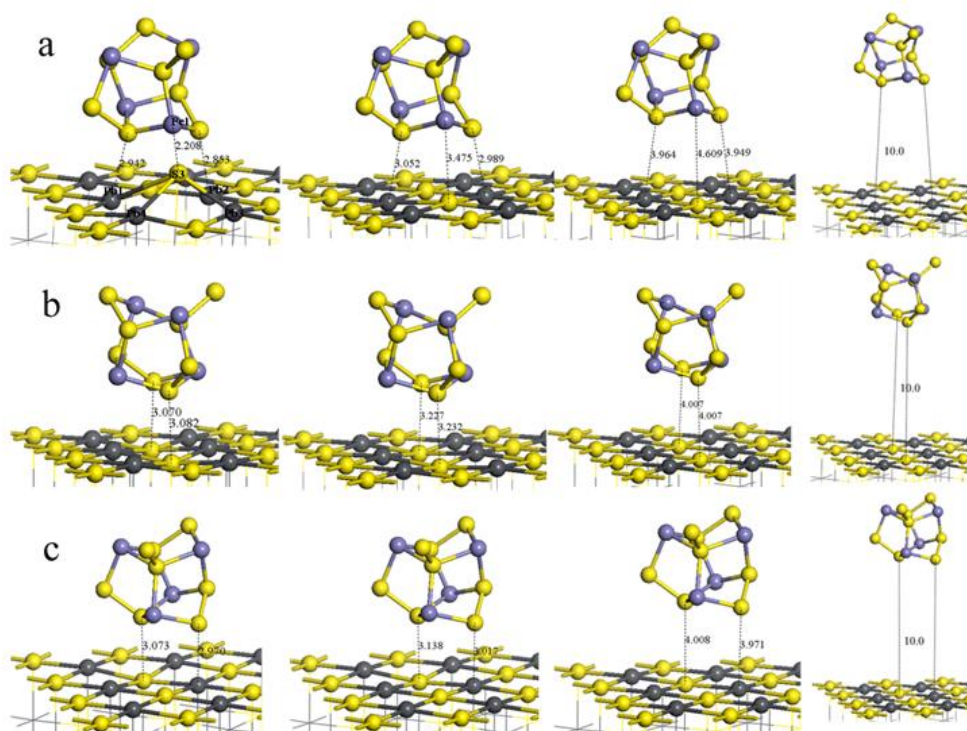


Fig. 3. Configurations of pyrite contact with (100) galena surface at (a) Pb-Pb site, (b) S-S site and (c) Pb-S site in different contact distances

It is found that when the contact distance is larger than 3 Å, the S-S site has the largest number of transferred electrons, followed by the Pb-S site contact, and then the Pb-Pb site contact. This result means that the galvanic interaction occurring at the S-S site is stronger than that occurring at other sites when the contact distance is larger than 3 Å. However, Fig. 2 shows that the number of transferred electrons at the Pb-Pb site shows a sharp increase at the contact distance of 3 Å, and at this point, the number of transferred electrons (0.33 e) is even larger than that at the S-S and Pb-S sites. This result indicates that the galvanic interactions occurring on the Pb-Pb site at the short contact distance are the strongest.

This strong galvanic interaction at the Pb-Pb site can be attributed to the interaction of pyrite Fe1 atom and galena S3 atom, as shown in Fig. 3(a). It is shown that the distance between the Fe1 atom and S3 atom is 2.208 Å, which is lower than the sum of the Fe atom and S atomic radii (2.30 Å), indicating the bonding between the Fe1 and S3 atoms. Moreover, it can be seen that the distance between the S3 atom and the Pb1 and Pb2 atoms are 3.881 and 3.792 Å, respectively, which are much larger than the sum of the Pb and S atomic radii (2.79 Å), indicating that these Pb-S bonds are broken. On the other hand, the distances between the S3 atom and the Pb3 and Pb4 atoms are 2.899 and 2.967 Å, respectively, indicating that Pb3 and Pb4 atom are still bonded to the S3 atom on the galena surface. However, at the Pb-S and S-S contact sites, the Fe atom of pyrite could not bond with the S atom on the galena surface at all of the contact distances. These results suggest that the galvanic interaction occurring at the Pb-Pb site with the contact distance of 3 Å could greatly enhance the S atomic relaxation and further enhance the oxidation of the galena surface.

It is also noted that when the contact distance is 10 Å, no electron transfer occurred on the pyrite and galena surface at all contact sites, implying that there is no galvanic interaction between pyrite and galena surfaces at the contact distance of 10 Å.

### 3.2 Effect of galvanic contact distance and contact site on the xanthate adsorption

The Pb-Pb site has been known as the most stable adsorption site of xanthate on the galena surface (Lan, 2012) so it has been selected as the adsorption site of xanthate on the galena surface in this research (as shown in Fig. 5). In the present study, different galvanic contact sites and distances were investigated to obtain the effects of galvanic interaction on the adsorption of xanthate on the galena surface. The adsorption energies are shown in Fig. 4, and the adsorption configurations are shown in Fig. 5.

Fig. 4 shows that the adsorption energy of xanthate decreases with the decrease of the contact distance at all contact sites. When the distance is larger than 4 Å, the adsorption energy decreases slowly. In these conditions, the Pb-Pb contact site has the highest adsorption energies, followed by the Pb-S contact site, and the S-S contact site has the lowest adsorption energies. However, when the distance is lower than 4 Å, the adsorption energies decrease significantly. It is found that the adsorption energy of Pb-Pb contact site is dramatically decreased and is even lower than that of the Pb-S and S-S sites at the contact distance of 3 Å. This could be attributed to the galvanic interaction between pyrite and galena surface being strongest at the Pb-Pb site.

It can be seen that the changes of adsorption energies (Fig. 4) correspond well to the changes in the number of transferred electrons (Fig. 2): the larger the electron transfer number (indicating the stronger galvanic interaction), the lower the adsorption energy (the stronger xanthate adsorption). Hence, the galvanic interaction between pyrite and galena surface can greatly enhance the adsorption of xanthate on the galena surface.

The Pb5-S4 bond lengths of xanthate adsorbed on galena surface are also shown in Fig. 5, and it can be seen that the S atoms of xanthate could bond with the Pb atoms of the galena surface at all contact sites and contact distances. Moreover, the Pb5-S4 bond lengths for the contact distance of 3 Å are less than those for the contact distance of 10 Å at the same contact site. It can also be seen that the Pb5-S4 bond lengths of more intense galvanic interaction model (Fig. 5(a)) are smaller than those of the weaker galvanic interaction model (Figs. 5(b) and 5(c)). Moreover, the changes of Pb6-S5 bond lengths are not obvious compared to the changes of Pb5-S4 bond lengths. These results indicate that the galvanic interaction could enhance the bonding strength of xanthate adsorbed on galena surface.

For a further study the xanthate adsorption, the density of states (DOS) of the Pb5-S4 bond at different contact sites and contact distances are shown in Fig. 6. It has been known that there is no galvanic interaction between pyrite and galena surface at the contact distance of 10 Å (shown in Fig. 2). Fig. 6 shows that these are mainly the S 3p, Pb 6s and Pb 6p DOS appear in the Fermi level. In addition, as shown in Fig. 6(a), with the contact distance change from 10 Å to 3 Å at Pb-Pb contact site, the DOS of S 3p and Pb 6p near Fermi level decrease sharply, indicating that at Pb-Pb contact site the bonding of Pb5 atom and S4 atom make the energy near Fermi level obviously reduce, which causing the structure become more stable.

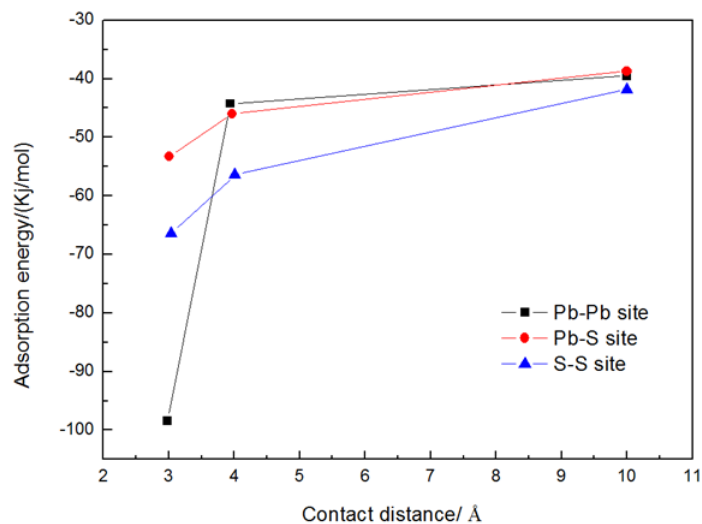


Fig. 4. Adsorption energy of xanthate on galena surface with galvanic contacting with pyrite at different contact sites and contact distances

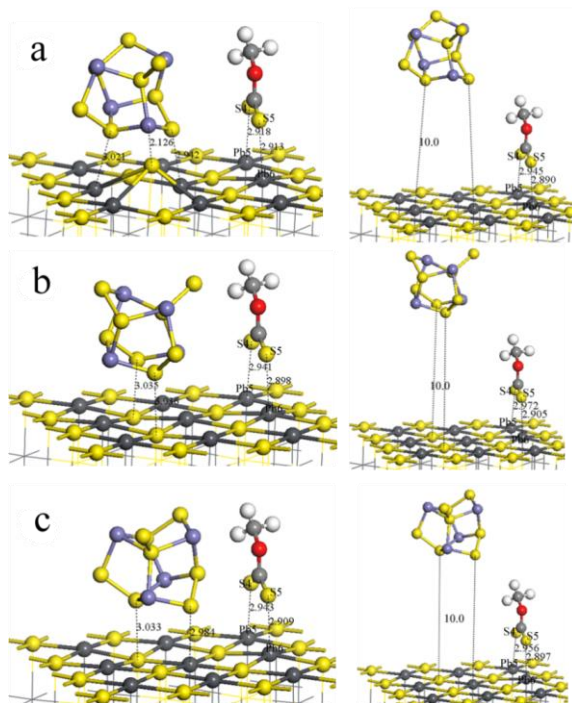


Fig. 5. Adsorption configurations of xanthate adsorbed on galena surface with galvanic contact with pyrite at the contact site of (a) Pb-Pb site, (b) S-S site and (c) Pb-S site with different contact distances

Moreover, the bonding range for Pb5 6p and S4 3p are in the valence band near the Fermi level. Particularly, Fig. 6 (a) shows that the bonding range for Pb5 6p and S4 3p at the distance of 3 Å

remarkably shifts to negative energy compared to that at the distance of 10 Å at the Pb-Pb contact site, and the non-locality of the S4 3p state is obviously enhanced in the range of -3 to 1 eV when the galvanic interactions occur. These results indicate that the Pb5-S4 bond at 3 Å contact distance is more stable than that at 10 Å contact distance, and the galvanic interaction enhances the bonding of Pb5 and S4 atoms at the Pb-Pb contact site. Fig. 6(b) shows that the bonding range for Pb5 6p and S4 3p at the S-S contact site shifts to negative energy and the non-locality of the S4 3p states is enhanced in the range of -3 to 1 eV with the occurrence of the galvanic interaction. Fig. 6(c) shows that the bonding range for Pb5 6p and S4 3p at Pb-S contact site shifts slightly to negative energy in the presence of the galvanic interaction.

Fig. 6 also shows that the density of states of the Pb5-S4 bond at the S-S, Pb-S and Pb-Pb contact sites are similar when the contact distance is 10 Å. However, when the contact distance is 3 Å, the negative shift of the Pb5-S4 bonding range and DOS non-locality at the Pb-Pb contact site are greatest, followed by that at the S-S contact site and that of the Pb-S contact site is the smallest, meaning that the Pb-S bond forming by xanthate and galena surface at the Pb-Pb site is stronger than that at the S-S or Pb-S contact sites.

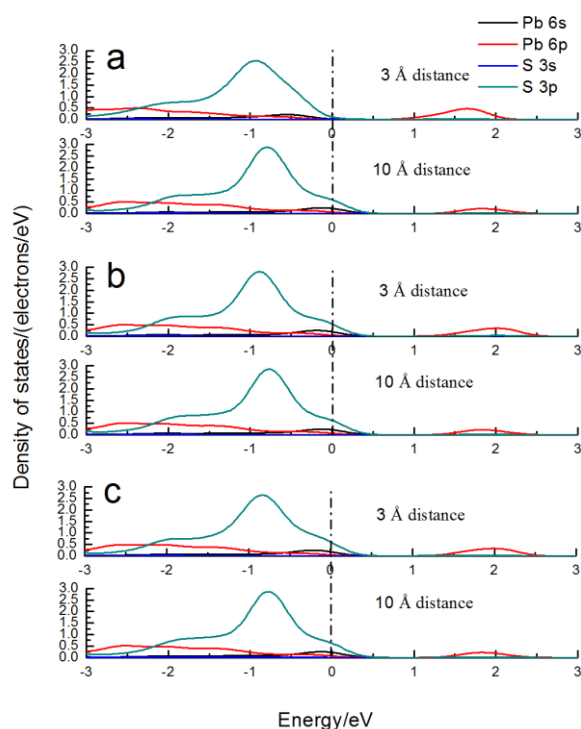


Fig. 6. Density of states of Pb5-S4 bond at (a) Pb-Pb contact site, (b) S-S contact site and (c) Pb-S contact site with different contact distances

A (6×3×1) supercell model of galena surface has also been constructed for investigating the adsorption site of xanthate which is farther away from pyrite. The adsorption site of xanthate on galena surface is still the Pb-Pb site. The adsorption configurations are shown in Fig. 7 and the adsorption energies are shown in Table 2.

Fig. 7 shows that the length of the Pb-S bond between xanthate and galena surface is 2.914 and 2.865 Å in the distance of 8.97 Å and that of bond length is 2.944 and 2.889 Å in the distance of 4.56 Å. These results indicate that the xanthate could adsorb on galena surface in both of the distances.

Table 2 shows that the adsorption energy of xanthate adsorbed on galena surface with the distance between pyrite and xanthate of 4.56 Å (-67.55 KJ/mol) is less than that of 8.97 Å (-58.69 KJ/mol), which indicates that the xanthate is more favour to adsorb on the galena surface at the distance between pyrite and xanthate of 4.56 Å than that of 8.97 Å. It may be attributed to the effect of galvanic interaction is weakened when far away from the galvanic contact site (the site pyrite contact with galena surface), and the adsorption energy of 8.97 Å (-58.69 KJ/mol) is closer to that without galvanic interaction (Fig. 4, -41.81 KJ/mol).



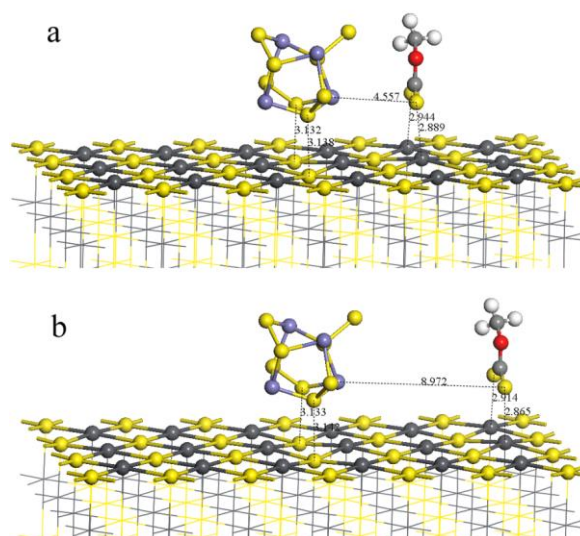


Fig. 7. Adsorption configurations of xanthate adsorbed on galena surface with the distance of (a) 4.56 Å and (b) 8.97 Å

Table 2. Adsorption energies of xanthate adsorbed on galena surface at different distances between pyrite and xanthate

| Distance between pyrite and xanthate/ Å | Adsorption energy/KJ/mol |
|---|--------------------------|
| 4.56                                    | -67.55                   |
| 8.97                                    | -58.69                   |

### 3.3 Cyclic voltammetric curves of galena and pyrite affected by galvanic interaction with the presence of butyl xanthate

Cyclic voltammetry measurements were first conducted on glassy carbon electrodes of powder galena, pyrite as well as mixture of galena and pyrite in a 1:1 weight ratio in the butyl xanthate concentration of 0.001 mol/dm<sup>3</sup> at pH 9.18. The results are shown in Fig. 8. Two oxidation peaks (peaks 1 and 2) are observed in the curves. Peak 1 that occurs near 100 mV is gentle, while peak 2, which occurs near 400 mV, is a strong oxidation peak. It can be seen that peak 1 of the mixed electrode occurs at the lower potential than that of pure pyrite or pure galena. The intensity of peak 2 for mixed electrode increased compared to galena and pyrite electrodes, indicating that the adsorption of xanthate on the mixed electrode is improved. Moreover, peak 2 of mixed electrode occurs at lower potential compared to galena and pyrite, meaning that it is easier for the adsorption of xanthate to occur on the mixed electrode, and the intensity of peak 2 of the mixed electrode is significantly enhanced compare to that of galena or pyrite, indicating that the galvanic interaction enhanced the xanthate adsorption.

To further investigate the galvanic interaction in detail, improved block electrodes are used, and the obtained CV results are shown in Fig. 9. As suggested in section 2.3, pyrite and galena are alternately used as electrodes for the measurement (electrode 1), and electrode 2 is used to study its galvanic effects on electrode 1. Here, in Fig. 9, the composition of electrode 1 is specified outside the parenthesis, and the composition of electrode 2 is specified inside the parenthesis. Two oxidation peaks (peaks 1 and 2) are found for both galena(galena) and galena(pyrite) curves in Fig. 9(a). It is obvious that the intensities of peaks 1 and 2 for the galena(pyrite) curve are stronger than those for the galena(galena) curve. In addition, the initial oxidation potential for the galena(pyrite) curve is lower than that for the galena(galena) curve. These results suggest that the adsorption of xanthate on the galena surface is increased due to the presence of pyrite. In the case of the measurement for the pyrite electrode (Fig. 9(b)), two oxidation peaks (peaks 3 and 4) and one reduction peak (peak 5) are found for the pyrite(pyrite) curve, while peak 3 disappears for the pyrite(galena) curve. Near 100mV, the initial potential of peak 4 shifts to the higher potential side with the presence of galena, suggesting



that the adsorption of xanthate on pyrite surface is decreased owing to the presence of galena. Based on the above results, it is clear that the galvanic interaction between galena and pyrite could improve the adsorption of xanthate on the galena surface while weakening the adsorption of xanthate on the pyrite surface. The DFT results have shown that the stronger the galvanic interaction the stronger the xanthate adsorption on galena, in good agreement with the cyclic voltammetric results.

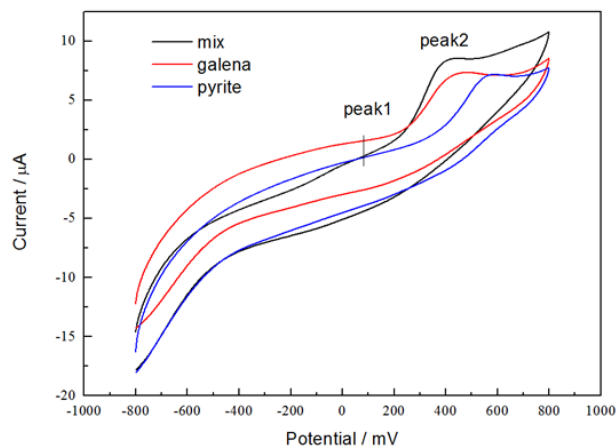


Fig. 8. Cyclic voltammetric curves of galena, pyrite and the mixture of galena and pyrite in the weight ratio of 1:1 glassy carbon electrodes in a buffer solution ( $0.01 \text{ mol/dm}^3$  sodium borate) at pH 9.18 and butyl xanthate concentration of  $0.001 \text{ mol/dm}^3$ . Scan rate  $V = 100 \text{ mV/s}$

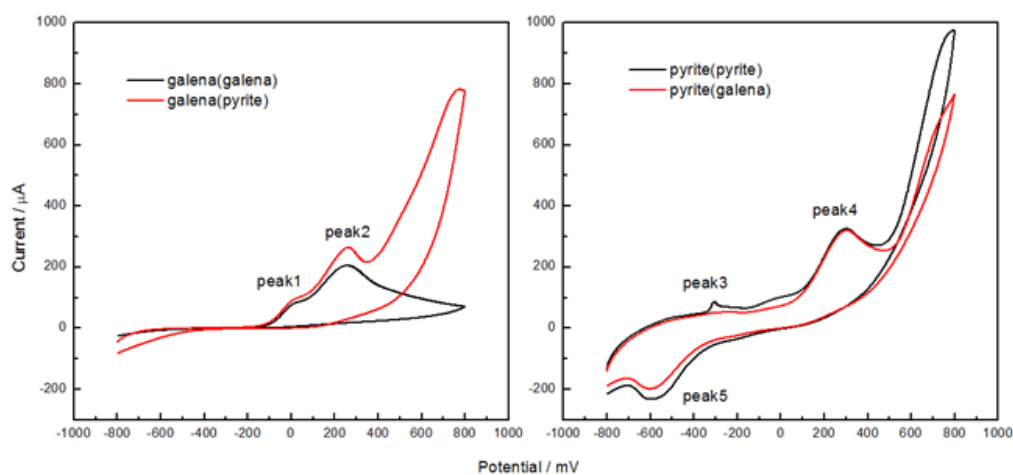


Fig. 9. Cyclic voltammetric curve of modified block electrodes in a buffer solution ( $0.01 \text{ mol/dm}^3$  sodium borate) at pH 9.18 and butyl xanthate concentration of  $0.01 \text{ mol/dm}^3$ . Scan rate  $V = 100 \text{ mV/s}$

#### 4. Conclusions

The number of transferred electrons changes with the change of the contact site between galena and pyrite; in particular, a sharp increase in the amount of the transferred electrons transfer number occurs at the Pb-Pb contact site at the contact distance of  $3 \text{ \AA}$ , enhancing the relaxation of S atoms on the galena surface and further improving the oxidation of the galena surface.

The adsorption energy of xanthate decreases with the increase of contact distance at all contact sites. Especially, when the distance is lower than  $4 \text{ \AA}$ , the adsorption energies decrease significantly, and the adsorption energy of the Pb-Pb contact site is dramatically decreased and becomes the lowest. The change in the adsorption energies corresponds well to the change in the number of the transferred electrons number: the stronger the galvanic interaction (larger amount of transferred electrons), the stronger the xanthate adsorption (lower adsorption energy), and the obtained results for the Pb-S

bond length and the density of states of the Pb-S bond are also in agreement with this trend. These results suggest that the galvanic interactions could improve the adsorption of xanthate on the galena surface. The cyclic voltammetry measurements also reveal that the galvanic interaction between galena and pyrite improves the adsorption of xanthate on the galena surface, in good agreement with the DFT results.

### Acknowledgments

The authors are grateful for the financial support provided by the National Natural Science Foundation of China (NSFC) (Grants No.51574092 and No.51364002) and the Found of State Key Laboratory of Mineral Processing (BGRIMM-KJSKL-2017-03).

### References

- IONESCU, A., ALLOUCHE, A., AYCARD J.P., RAJZMANN, M., GALL, R.L., 2003. *Study of  $\gamma$ -Alumina-Supported Hydrotreating Catalyst: I. Adsorption of Bare MoS<sub>2</sub> Sheets on  $\gamma$ -Alumina Surfaces*. J. Phys. Chem. B 107, 8490-8497.
- CHEN, J., KE, B., LAN, L., LI, Y., 2015. *Influence of Ag, Sb, Bi and Zn impurities on electrochemical and flotation behaviour of galena*. Miner. Eng. 72, 10-16.
- CHENG, X., IWASAKI, I., 1992. *Effect of chalcopyrite and pyrrhotite interaction on flotation separation*. Miner. Metall. Proc. 9, 73-79.
- CHMIELEWSKI, T., KALETA, R., 2011. *Galvanic Interactions of Sulfide Minerals in Leaching of Flotation Concentrate from Lubin Concentrator*. Physicochem. Probl. M. 21-34.
- EKMEKÇI, Z., DEMIREL, H., 1997. *Effects of galvanic interaction on collectorless flotation behaviour of chalcopyrite and pyrite*. International Journal of Mineral Processing 52, 31-48.
- HEIDMANN, I., CALMANO, W., 2010. *Removal of Ni, Cu and Cr from a galvanic wastewater in an electrocoagulation system with Fe- and Al-electrodes*. Sep Purif Technol 71, 308-314.
- HERBERT, F.W., KRISHNAMOORTHY, A., MA, W., VLIET, K.J.V., YILDIZ, B., 2014. *Dynamics of point defect formation, clustering and pit initiation on the pyrite surface*. Electrochim Acta 127, 416-426.
- KE, B., LI, Y., CHEN, J., ZHAO, C., CHEN, Y., 2016. *DFT study on the galvanic interaction between pyrite (100) and galena (100) surfaces*. Applied Surface Science 367, 270-276.
- LAN, L., 2012. *The effect of lattice defect of galena on the surface property, molecular absorption of flotation reagents and electrochemical behavior*. Guangxi university.
- LI, J., CROISSET, E., RICARDEZSANDOVAL, L., 2013. *Effect of Metal-Support Interface During CH<sub>4</sub> and H<sub>2</sub> Dissociation on Ni/ $\gamma$ -Al<sub>2</sub>O<sub>3</sub>: A Density Functional Theory Study*. J. Phys. Chem. C, 117, 16907-16920.
- LI, Y., CHEN, J., CHEN, Y., ZHAO, C., ZHANG, Y., KE, B., 2018. *Interactions of Oxygen and Water Molecules with Pyrite Surface: A New Insight*. Langmuir 34, 1941-1952.
- LIU, Q.Y., HE-PING, L.I., ZHOU, L., 2007. *The Study on the Galvanic Effect of Sulphide Minerals: A Review*. Bulletin of Mineralogy Petrology & Geochemistry 26, 284-289.
- LIU, Q.Y., LI, H.P., ZHOU, L., 2009. *Experimental study of pyrite-galena mixed potential in a flowing system and its applied implications*. Hydrometallurgy 96, 132-139.
- MONKHORST, HENDRIK, J., JAMES, D., 1976. *Special points for Brillouin-zone integrations*. Physical Review B 13, 5188-5192.
- MOSLEMI, H., SHAMSI, P., HABASHI, F., 2011. *Pyrite and pyrrhotite open circuit potentials study: Effects on flotation*. Miner Eng 24, 1038-1045.
- NOOSHABADI, A.J., RAO, K.H., 2014. *Formation of hydrogen peroxide by sulphide minerals*. Hydrometallurgy 141, 82-88.
- PERDEW, J.P., CHEVARY, J.A., VOSKO, S.H., JACKSON, K.A., PEDERSON, M.R., SINGH, D.J., FIOLETTI, C., 1992. *Atoms, molecules, solids, and surfaces: Applications of the generalized gradient approximation for exchange and correlation*. Physical Review B Condensed Matter 46, 6671-6687.
- QIN, W.Q., WANG, X.J., LI-YUAN, M.A., JIAO, F., LIU, R.Z., GAO, K., 2015. *Effects of galvanic interaction between galena and pyrite on their flotation in the presence of butyl xanthate*. T. Nonferr. Metal Soc. 25, 3111-3118.
- RAO S R, F.J.A., 1988. *Galvanic Interaction Studies on Sulphide Minerals*. Canadian Metallurgical Quarterly 4, 253-259.
- ROSCIONI, O.M., DYKE, J.M., EVANS, J., 2013. *Structural Characterization of Supported RhI(CO)<sub>2</sub>/ $\gamma$ -Al<sub>2</sub>O<sub>3</sub> Catalysts by Periodic DFT Calculations*. Journal of Physical Chemistry C 117, 19464-19470.

- SADEGHAMIRSHAHIDI, M., KISH, T.E., ARDEJANI, F.D., 2013. *Application of Image Processing for Modelling Pyrite Oxidation in a Coal Washing Waste Pile*. *Environ Model Assess* 18, 365-376.
- SHANG, C., LIU, Z.P., 2010. *Is Transition Metal Oxide a Must? Moisture-Assisted Oxygen Activation in CO Oxidation on Gold/ $\gamma$ -Alumina*. *J. Phys. Chem. C*, 16989-16995.
- SILVA, G.D., LASTRA, M.R., BUDDEN, J.R., 2003. *Electrochemical passivation of sphalerite during bacterial oxidation in the presence of galena*. *Miner. Eng.* 16, 199-203.
- VANDERBILT, D., 1990. *Soft self-consistent pseudopotentials in a generalized eigenvalue formalism*. *Physical Review B Condensed Matter* 41, 7892-7895.
- ZHANG, R., LIU, H., WANG, B., LING, L., 2012. *Insights into the effect of surface hydroxyls on CO<sub>2</sub> hydrogenation over Pd/ $\gamma$ -Al<sub>2</sub>O<sub>3</sub> catalyst: A computational study*. *Applied Catalysis B Environmental* 126, 108-120.